Soft Matter

Accepted Manuscript

ROYAL SOCIETY OF CHEMISTRY

www.rsc.org/softmatter

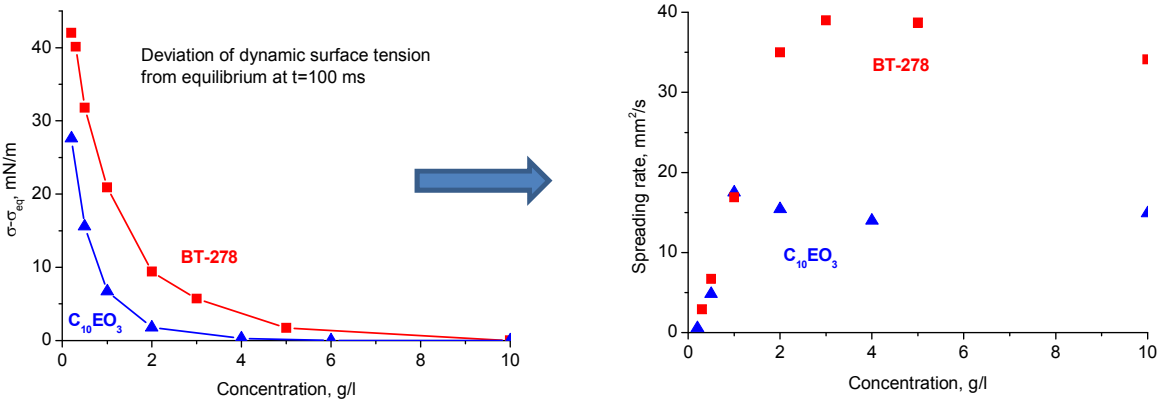

Effect of adsorption kinetics on the rate of surfactant-enhanced spreading

N.M. Kovalchuk[1,2],O.K. Matar[1], R.V. Craster[1], R.Miller[3], V.M. Starov*[4]
[1]Imperial College London, South Kensington Campus, London SW7 2AZ, UK
[2]Institute of Biocolloid Chemistry, Kiev, 03142, Ukraine
[3]Max Planck Institute of Colloids and Interfaces, Golm, D-14424, Germany
[4]Loughborough University, Loughborough, LE 11 3TU, UK
*Corresponding author: e-mail V.M.Starov@lboro.ac.uk

A comparison of the kinetics of spreading of aqueous solutions of two different surfactants on the identical substrate and their short time adsorption kinetics at the water/air interface has shown that the surfactant which adsorbs slower provides a higher spreading rate. This observation indicates that Marangoni flow should be an important part of the spreading mechanism enabling surfactant solutions to spread much faster than pure liquids with comparable viscosities and surface tensions.

Surfactants are broadly used to improve the spreading performance of aqueous formulations on hydrophobic substrates. The effectiveness of surfactant in facilitating wetting depends on its ability to lower the liquid-air and solid-liquid interfacial tensions. As a rule for hydrocarbon-based surfactants the lower liquid-air interfacial tension corresponds to better wetting properties. However, aqueous solutions of fluoro-surfactants despite their low surface tension are less effective in the wetting of hydrocarbon-based hydrophobic substrates because of their lower affinity to hydrocarbons [1]. The trisiloxane surfactants provide the best spreading performance enabling complete wetting of highly-hydrophobic substrates such as polypropylene and parafilm [2,3]. Mixed solutions of cationic and anionic surfactants (catanionic mixtures) can wet polyethylene film [4,5]. Substrates possessing higher surface energy are wetted completely by aqueous solutions of ethoxylated alcohols [6], sodiumbis(2-ethylhexyl) sulfosuccinate (AOT) and didodecyldimethylammonium bromide [7].

If it is assumed that the identical mechanism governs the spreading of pure liquids and surfactant solutions, then it can be expected that surfactants solutions spread at the same rate as pure liquids or even slower in the case wherein the characteristic timescale of adsorption is larger than that of spreading. However, numerous experimental studies have shown that surfactant solutions can spread much faster than pure liquids on the identical substrates with the spreading area, S, being proportional to time, $S \sim t$ [2,3] as compared to $S \sim t^{0.2}$ for pure liquids [8,9]. Therefore, there must be additional mechanisms facilitating the fast spreading of surfactant solutions. The most probable candidates are: the ‘caterpillar-like’ motion at the

moving three-phase contact line, providing lower energy dissipation [10]; bilayer formation at the leading edge of spreading [11,12]; and Marangoni flow [13,14]. The comprehensive discussion on all these mechanisms is given in Ref [15].

Below the relevance of Marangoni flow as one of the mechanisms of surfactant-enhanced spreading is addressed. This mechanism looks very promising, considering the fundamental difference between the surface of pure liquids and that of surfactant solutions. The surface tension of a pure liquid under isothermal dynamic conditions is identical over the entire liquid-air interface. The adsorbed surfactant layer, however, possesses visco-elasticity [16], i.e. the surface tension decreases by contraction and increases by expansion of the surface and the changes in the surface tension depend on the rate of deformation and the rate of surfactant exchange between the liquid bulk and the interface, in particular on the diffusion of the surfactant monomers from the bulk to the interface. Other processes influencing dynamic surface tension are diffusion and disintegration of aggregates in the bulk of liquid, surface diffusion and convection as well as reorientation and rearrangement of adsorbed molecules. Dynamics of these processes is discussed for example in [17,18]. The rate of surfactant transfer to the interface depends also on convective patterns inside the spreading droplet. The faster is convective flow along the interface the thinner is diffusion boundary layer, i.e. the diffusion time scale decreases with an increase of convective velocity [19]. Considering the processes in the close vicinity of the three phase contact line, a large surface curvature here can also affect the time scale of diffusion mass transfer [18,20]. That is, the surface tension under dynamic conditions can be considerably different from the equilibrium value. The difference increases with an increase of the deformation rate and a decrease of surfactant concentration.

The surface expands very quickly during the spreading with typical spreading rates being of order of tens of mm^2/s. Therefore, it is possible to assume that at the leading edge of spreading the surface tension becomes higher than that near the droplet apex. This difference in the surface tensions gives rise to Marangoni flow in the direction of spreading facilitating in this way the spreading process, as it is shown in Fig. 1, where the direction of Marangoni flow at the surface is shown by arrows. It is important to note that in order to create a sufficiently large gradient the surface tension at the droplet apex should remain close to the equilibrium value. This becomes increasingly difficult to achieve with decreasing concentration, which explains why the spreading rate exhibits a maximum vs. concentration [13].

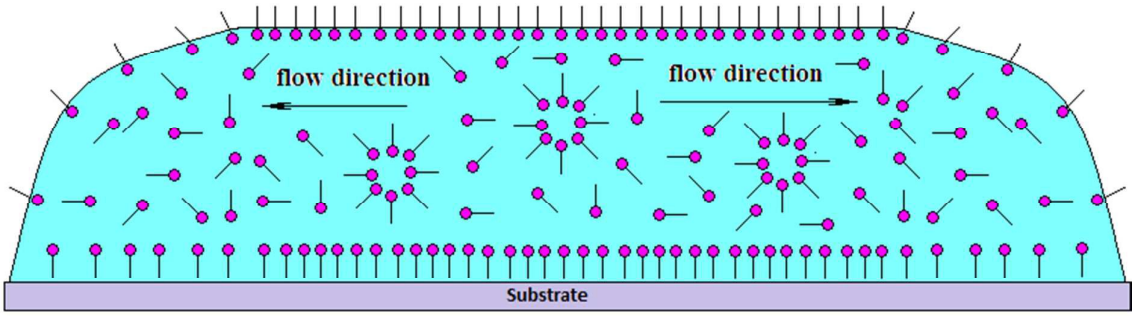

Fig. 1. Schematic representation of spreading droplet of surfactant solution with Marangoni flow due to difference in the surface concentration facilitating spreading.

The surface tension at the leading edge of a spreading drop is determined by the ratio of the characteristic timescale of interfacial expansion and that of adsorption: the slower the adsorption rate the higher the surface tension at the same rate of interfacial expansion. Therefore, if the Marangoni flow contributes significantly to the mechanism of surfactant-enhanced spreading then a surfactant solution with a low adsorption rate allows surface tension gradients to be sustained for longer time giving rise to a rapid spreading.

To prove the hypothesis that Marangoni flow is an essential component of the mechanism of surfactant-enhanced spreading, a comparative study on the spreading and adsorption of aqueous solutions of triethylene glycol monodecyl ether, $C_{10}EO_3$, (Fluka, >97%) and trisiloxane surfactant BREAK-THRU S 278,BT-278, (Evonik) was performed under the identical experimental conditions. The chemical structure of BT-278 can be represented as $M(D'EO_{7.5}OMe)M$, where M is the trimethylsiloxy group $(CH_3)_3SiO_{1/2}$–, D' is $O_{1/2}Si(CH_3)(CH_2)_3O_{1/2}$, EO is the oxyethylene group (-O-CH2-CH2), and Me stands for the end-capping group $O\text{-}CH_3$. The surfactants solutions used in this study have the viscosity equal to the viscosity of water; therefore the viscous dissipation at similar conditions is the same and does not influence the spreading kinetics.

The isotherms of surface tension of the surfactants under investigation are presented in Fig. 2. Only the regions of the surface tension isotherms close to the Critical Aggregation Concentration (CAC) have been measured, because complete wetting by surfactants solutions occurs solely at concentrations above the CAC. For BT-278, complete wetting is observed at concentrations above 2.5 CAC. This concentration is referred to as Critical Wetting Concentration (CWC); for $C_{10}EO_3$ CWC equals the CAC.

Fig. 2 show that both surfactants have rather close values of CAC, around 0.1 g/l (CWC~0.25 g/l) for BT-278 and 0.2 g/l for $C_{10}EO_3$. All experiments in the presented study have been performed at concentrations equal to or greater than the CWC to ensure we are in the regime of complete wetting. As the values of CWC in g/l are close for the two surfactants under consideration, the mass concentration is more convenient for comparison of their properties. The reference to concentration in CWC (CAC) units is also given below.

Fig. 2 also shows that the solutions of BT-278 provide lower surface tension (~22 mN/m) as compared to the solutions of $C_{10}EO_3$ (~27 mN/m) at concentrations above CAC. Because of the relatively high surface tension $C_{10}EO_3$ demonstrates only partial wetting on such substrates as polyethylene, propylene and parafilm. To achieve complete wetting the substrate roughness was used as a factor facilitating wetting. According to the Wenzel equation [21] $\cos(\theta_W) = r\cos(\theta_Y)$, where θ_Y is the Young contact angle measured on a smooth substrate, θ_W is the Wenzel contact angle on a rough substrate, and r is the ratio of the actual surface area to the projected area, increasing with the increase of substrate roughness. Therefore in the case of $\theta_Y<90°$, complete wetting occurs at $r>1/\cos(\theta_Y)$. Another reason for better wetting of a rough substrate is the capillary condensation: according to [22] the rough surface is wetter in comparison to the smooth one at the same ambient humidity due to capillary condensation inside the grooves. Complete wetting for solutions of both surfactants was achieved using Polyvinyl idene fluoride, PVDF, film, thickness 0.05 mm (GoodFellow), roughness R_{rms}= 530 ± 2 nm (AFM, scan size 80 μm). The contact angle of water on PVDF films was 84±2 °.

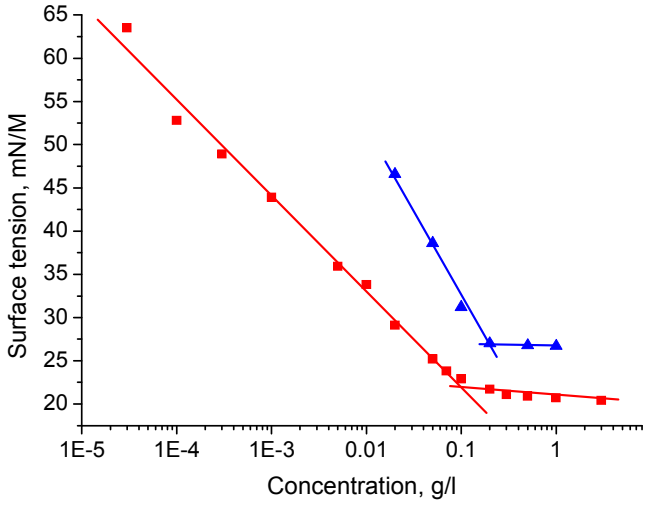

Fig. 2. Surface tension vs concentration for BT-278 (squares), and $C_{10}EO_3$ (triangles). For each surfactant, lines are the best linear fit shown for the isotherms in concentration ranges above and below the Critical Aggregation Concentration.

The contact angle and equilibrium surface tension were measured with a DSA-100 instrument (Krüss) using the bubble/drop shape analysis. The short-time dynamic surface tension was measured with BPA-1P tensiometer (SINTERFACE) which is based on the Maximum Bubble Pressure method.

All spreading experiments were performed at room temperature, T=23±1°C, and relative humidity (RH) of 40±5. The kinetics of spreading was measured using the series of images of spreading droplets of volume 2 µl (top view) taken by a video camera at 15 fps. The spreading area was calculated for selected images using the ImageJ free software. The spreading factor was calculated as a ratio of the maximum spreading area and the area covered by a droplet of pure water of the same volume using snapshots of the spread droplets. The droplets of volume 5µl were used. The experimental error was inside 20 % for all measurements of spreading area.

The experimental results on the spreading kinetics are presented in Fig. 3 demonstrating that the spreading exponent is still lower than 1 (but essentially higher than 0.2) at concentrations close to CWC. A linear dependence of the spread area on time, however, was observed already at a concentration of 0.5 g/l (2.5 CWC) for $C_{10}EO_3$ and 1 g/l (4 CWC) for BT-278. Upon further increase of the concentration the linear dependence of the spreading area on time with weak dependence of spreading rate on concentration was observed at the initial stage of spreading. However, subsequent spreading decelerates considerably in relation to the spreading observed at lower concentrations. The deceleration begins at earlier times with increasing concentration. Similar deceleration was also observed at spreading of catanionic mixtures on polyethylene substrate [5].

It should be emphasised that the deceleration was observed only in spreading experiments performed at room humidity. Its reason and dependence on the concentration is to be revealed and further thorough study including experiments at various humidities is required to understand the mechanism governing the deceleration. However, from the results presented in Fig. 3 it is obvious that deceleration cannot be explained by the effect of evaporation. Spreading of solutions of higher concentrations decelerated at relatively small spread area, whereas spreading of less concentrated solutions proceeded further despite the increase of evaporative flux which is proportional to the radius (i.e. the larger is the radius of spread droplet the most important is evaporation). It should be also noted that after deceleration in the spreading of highly concentrated solutions the spread area remained constant during at least 10 seconds, that is evaporation at this time scale

can be neglected at spread areas below 100 mm^2. At the same time in the case of larger final spread areas (smaller concentrations) the maximum spread area retained only ~1 s and then started to retract due to evaporation.

From the time scales mentioned above it can be also concluded that evaporation hardly influences the surfactant distribution inside the spreading droplet, at least during the initial 2-3 seconds of spreading, when the power law $t^{0.5}$ is already observed. It is well known that the evaporation has the maximum intensity near the three phase contact line. It is proposed in [23] that the main reason for this is the temperature difference of the drop surface: the thickness of the drop has minimum near the contact line, therefore the temperature here is highest due to thermal exchange with substrate. In the case considered here the contact angle decreases very quickly and during the main part of spreading the drop has a shape of a pancake of thickness smaller than 0.1 mm (thickness 0.1 mm correspond to the spread area of 20 mm^2 in Fig. 3, i.e. t<1 s). For such thin films the instantaneous thermal equilibration with the substrate can be assumed.

The deceleration which commenced during the early stages of the spreading with increasing concentration mentioned above is the reason that the spreading area exhibits a maximum with respect to the concentration for the surfactant solutions studied in the present work as shown in Fig. 4. Similar dependence of the spreading area on the concentration was observed previously in the literature [5,24].The maximum spreading area was observed at the same concentration 1 g/l for both surfactants, but the maximum spreading factor was nearly a factor of two lower for $C_{10}EO_3$ solution as compared to BT-278 solution. The thickness of spread film is in the range of 11-57 μm for $C_{10}EO_3$ solutions and 6-35 μm for BT-278 solutions depending on concentration. It is important to note that in all previous studies the maximum in the spreading area was observed under conditions of the room humidity.

The spreading rate calculated as the slope of the linear part of the kinetic curves in Fig. 3 has a maximum at concentration 1 g/l (5 CWC) for $C_{10}EO_3$ and at concentration 3 g/l (12 CWC) for BT-278. The maximum spreading rate of the $C_{10}EO_3$ solution is ~17 mm^2/s, which is less than a half of that associated with the BT-278 solution (~39 mm^2/s). The characteristic time of spreading (and of relative interfacial expansion), τ, was estimated from relation $\frac{1}{\tau} = \frac{1}{S_0}\frac{dS}{dt}$ as τ~0.25 s for the BT-278 solutions and τ~0.500 s for the $C_{10}EO_3$ solutions, respectively; here, *t* is the time, *S* is the spreading area, S_0 is the initial area of the droplet. Note that the values of the characteristic time are most probably overestimated because they do not take into account the substrate roughness (the real increase of the solid-liquid interface is much higher than that of liquid/air interface). It is noteworthy that the characteristic time of spreading of BT-278 on smoother substrate, polyethylene film, is less than half of that on the rough substrate, τ~0.12 s, as estimated from the kinetics data presented in Ref. [5].

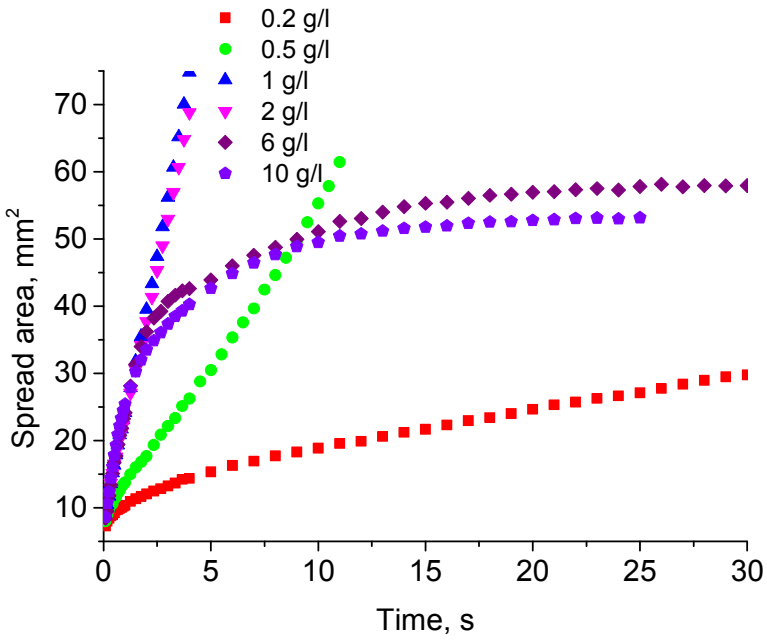

(a)

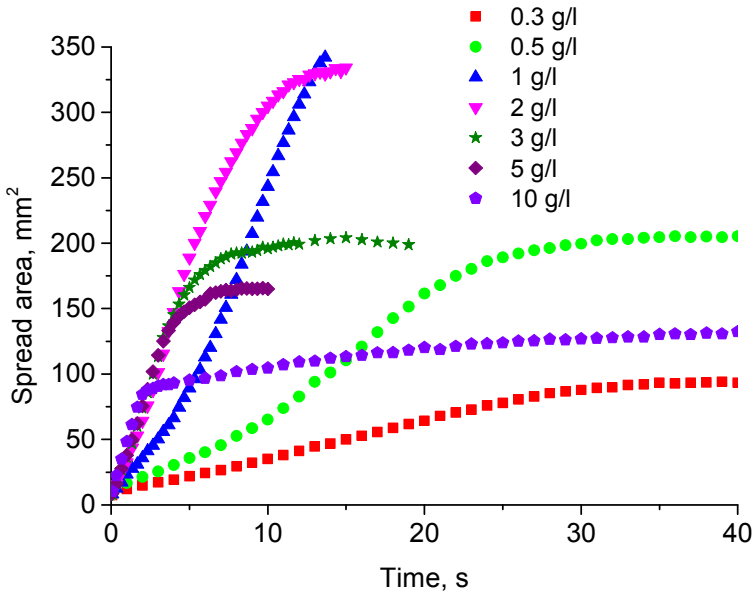

(b)

Fig. 3. Spreading kinetics for 2 µl droplet of: a – $C_{10}EO_3$ and b – BT-278 solutions.

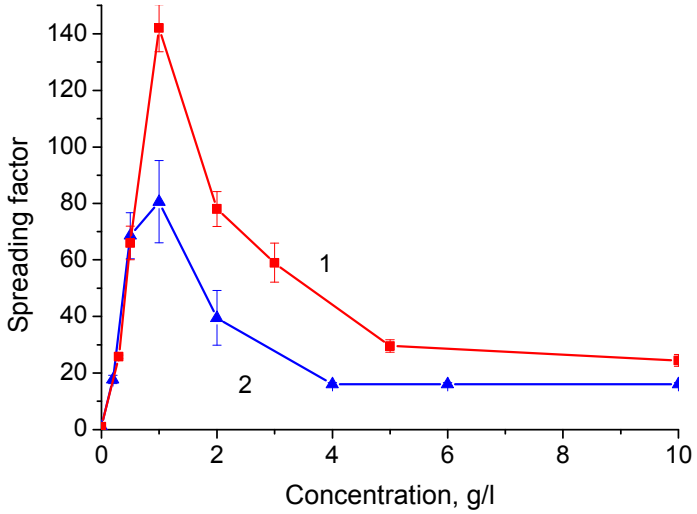

Fig. 4.Spreading factor vs concentration for a 5 μl droplet of BT-278 (squares) and $C_{10}EO_3$ (triangles).

The results for the short-time temporal evolution of the dynamic surface tension of a series of BT-278 and $C_{10}EO_3$ solutions are presented in Fig. 5. Note that for each surfactant the equilibrium surface tension is the same for all solutions as the measurements are performed at concentrations above CAC. It is seen from Fig. 5 that at the times corresponding to the characteristic time of spreading the dynamic surface tension is noticeably higher than the equilibrium surface tension for all concentrations where the fast spreading was observed, and the deviation from equilibrium is essentially higher for solutions of BT-278.

Fig. 6 shows the deviation from the equilibrium value of surface tension depending on concentration for two different times: 0.01 s and 0.1 s. In both cases for all concentrations the deviation from equilibrium is higher for solutions of BT-278, i.e. this surfactant demonstrates a slower adsorption kinetics at concentrations above CAC. It is clear that a higher deviation from the equilibrium can cause faster Marangoni flow in the case of BT-278 solutions for the reasons outlined above.

Another mechanism, which can increase the surfactant depletion at the leading edge of spreading and in this way accelerate the Marangoni convection is the depletion of aggregates from the leading edge of spreading. However considering that the thickness of spread film exceeds 6 μm=6000 nm in the very end of spreading process, whereas the maximum size of aggregates found in our measurements on BT-278 solutions using Malvern Zeta-sizer was around 250 nm, this mechanism looks rather improbable. Nevertheless micelles can be absent at the leading edge of

spreading, due to disintegration to replenish the monomer concentration depleted by adsorption on the newly created interfaces. The depletion in BT-278 solutions can also occur due to multilayer formation on the solid substrate, but the time scale of this process is larger than the time scale of spreading [25].

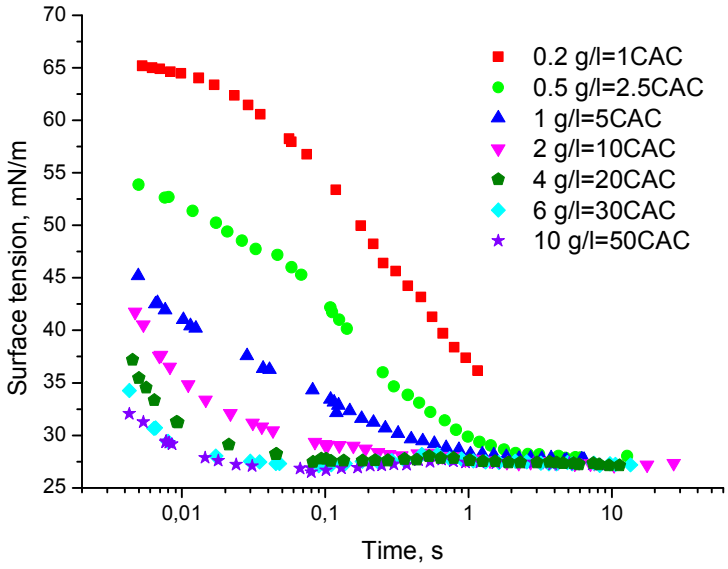

(a)

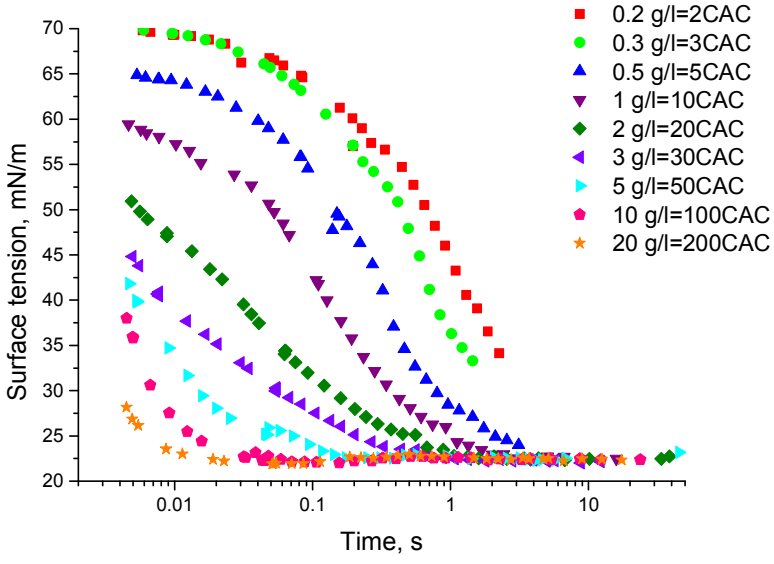

(b)

Fig. 5.Temporal evolution of the dynamic surface tension of $C_{10}EO_3$ (a) and BT-278 (b) solutions.

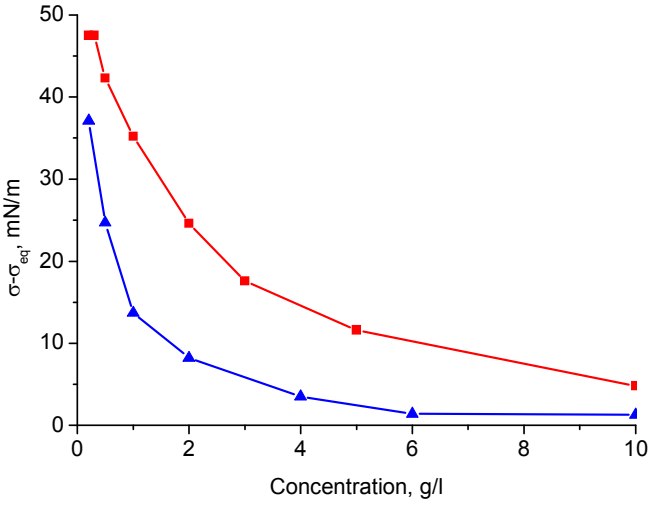

(a)

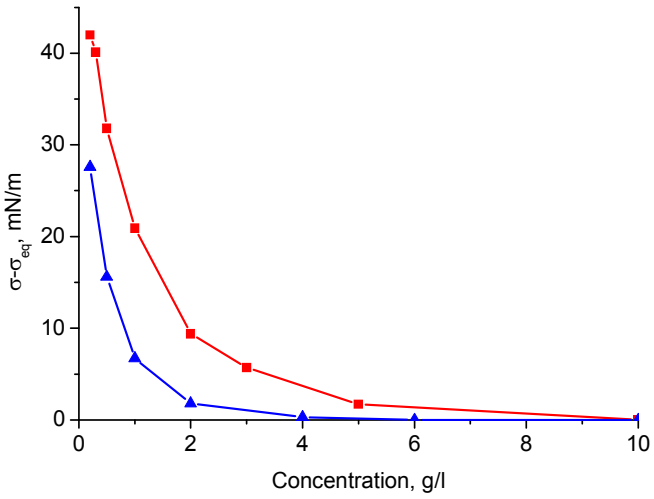

(b)

Fig. 6. Deviation of the surface tension from its equilibrium value at 0.01 s (a) and 0.1 s (b) for BT-278 (squares) and $C_{10}EO_3$(triangles).

Conclusions

The wetting and adsorption kinetics for solutions of two different surfactants: triethylene glycol monodecyl ether ($C_{10}EO_3$) and a trisiloxane superspreader (BT-278) are compared. The result of this comparison demonstrates that complete wetting is observed for both surfactants with a linear dependence of the spreading area on time. For both surfactants at room humidity the spreading decelerates after a certain time interval, duration of which decreases with increasing of surfactant concentration. The results also show that the spreading rates of BT-278 solutions are more than twice higher than those associated with $C_{10}EO_3$ solutions. It is found that the dynamic surface tension of both surfactants deviates significantly from its equilibrium value on timescales commensurate with those of the spreading process. The deviation is considarably larger in the case of BT-278. Taking into account that drops of BT-278 solution spread much faster than their $C_{10}EO_3$ counterparts, it can be concluded that Marangoni flow due to the gradient of surface tension (with a higher surface tension at the drop leading edge because of the slower surfactant supply from the bulk) should be an essential part of the mechanism of surfactant-enhanced spreading. This flow accelerates the spreading and contributes to the replenishment of the surfactant in the region of the advancing three-phase contact line. To further confirm the importance of Marangoni flow in the spreading of surfactant solutions thorough comparative studies are required, including experiments involving a broader range of surfactants and substrates.

Acknowledgments

This work was supported by Engineering and Physical Sciences Research Council, UK, grants EP/J010596/1, EP/D077869/1 and EP/L020564/1, by CoWet, Marie Curie EU project, by ESA under grants FASES and PASTA, and by COST MP1106 project. We would like to express special thanks to Dr. Joachim Venzmer (Evonic) for donating the surfactant BT-278. We also thank Dr. David Grandy for the AFM measurements.

References

1. N.M.Kovalchuk, A.Trybala, V.Starov, O. Matar, N. Ivanova, *Adv. Colloid Interface Sci*. 2014, **210**, 65.

2. R.M.Hill, *Curr.Op. Colloid Interface Sci.*, 1998, **3**, 247.

3. J.Venzmer, *Curr. Op. Colloid Interface Sci.*, 2011, **16**, 335.

4. Y. Wu, M.J. Rosen, *Langmuir*, 2005, **21**, 2342.

5. N.M. Kovalchuk, A. Barton, A. Trybala, V. Starov, Submitted to *J. Colloid Interface Sci*.

6. T.Stoebe, Z.Lin, R.M.Hill, M.D.Ward, H.T.Davis,*Langmuir*, 1997, *13*, 7270.

7. T.Stoebe, R.M.Hill,M.D.,Ward, H.T. Davis,*Langmuir*, 1997, **13**, 7276.

8. L.H. Tanner,*J. Phys. D: Appl. Phys.,* 1979, **12**, 1473.

9. V.M. Starov, V.V. Kalinin, J.D. Chen, *Adv. Colloid Interface Sci*., 1994, **50**, 187.

10. V.Starov, *Colloid. Polym.Sci*., 2013, **291**, 261.

11. E. Ruckenstein, *Colloid Surf. A*, 2012, **412**, 36.

12. P. Theodorakis, E.A. Muller, R.V. Craster, O.K. Matar, *Langmuir*, 2015, **31**, 2304.

13. A. Nikolov, D. Wasan, *Eur. Phys. J. Special topics*, 2011, **197**, 325.

14. G.Karapetsas, R.V.Craster, O.K. Matar,*J. Fluid Mech.* 2011, **670**, 5.

15. Kovalchuk N.M., Trybala A., Arjmandi-Tash O., Starov V. Adv. Coll. Int. Sci., 2015, doi: http://dx.doi.org/10.1016/j.cis.2015.08.001.

16. M. van den Tempel, J. Lucassen, E.H. Lucassen-Reynders, *J. Phys.Chem*., 1965, **69**, 1798.

17. S.S. Dukhin, G. Kretzschmar, R. Miller, Dynamics of adsorption at liquid interfaces: theory, experiment, applications. D. Mobius, R. Miller (Eds.), Studies in Interface science. Amsterdam: Elsevier, 1995.

18. P.Joos, *Dynamic surface phenomena*, VSP, Dordrecht, The Netherlands, 1999.

19. N.J. Alvarez, D.R. Vogus, L.M. Walker, S.L. Anna, *J. Coll. Int. Sci.*, 2012, **372**, 183.

20. N.J. Alvarez, L.M. Walker, S.L. Anna, Phys. Rev. E, 2010, 82, 011604.

21. A.Marmur, *Langmuir*, 2003, **19**, 8343.

22. Z.Lin, R.M.Hill, H.T.Davis, M.D. Ward, *Langmuir*, 1994, **10**, 4060.

23. V. Starov, K. Sefiane, Coll. Surf. A 2009, **333**, 170.

24. X. Wang., L. Chen, E. Bonaccurso, J. Venzmer, *Langmuir*, 2013, **29**, 14855.

25. N.A. Ivanova, N.M. Kovalchuk, V.D. Sobolev, V.M. Starov, Soft Matter, 2015, DOI: 10.1039/C5SM02043C.